© Universiti Tun Hussein Onn Malaysia Publisher's Office

IJIE

Journal homepage: http://penerbit.uthm.edu.my/ojs/index.php/ijie
ISSN : 2229-838X e-ISSN : 2600-7916

The International Journal of Integrated Engineering

Edge Detection using Ant Colony Optimization under Novel Intensity Mapping Function and Weighted Adaptive Threshold

Akshi Kumar[1], Sahil Raheja[2*]

[1]Dept. of Computer Science and Engineering,
Delhi Technological University, Delhi, INDIA

[1]Research Scholar, Department of Information Technology,
Delhi Technological University, Delhi, INDIA

*Corresponding Author

DOI: https://doi.org/10.30880/ijie.2020.12.01.002
Received 6 September 2018; Accepted 18 November 2018; Available online 31 January 2020

Abstract: Edge detection is a crucial phenomenon in image segmentation. In general, kernel based methods like Sobel, Canny, Roberts etc. are used which are based on first and second derivatives pixels intensity. However, these methods fail to find all the true edges. Moreover, number of falsely detected edges is much more than true edges. This happens due to a fixed threshold used in these methods. To reduce falsely detected edges, a method which can dynamically adjust its threshold is desirable. Artificial and swarm intelligence based methods are capable to handle minute details. In this work, Ant Colony Optimization (ACO) based method is detailed for edge detection. In this method, a novel function is used to capture intensity variation in a particular image. In learning based method adjustment of threshold is also necessary to obtain good results. In this work, we have considered weighted average for threshold update in contrast to earlier method where simple average is taken. The performance evaluation and comparison is made in terms of Peak-Signal-to Noise Ratio (PSNR), accuracy and FScore and usefulness of proposed method is shown. Finally, results are compared in terms of F-score with recent methods. In the earlier compared method Sketch Token provide best F-score of 0.73 and with proposed method the obtained best F-score is 0. 97, therefore percentage improvement is of 32.80% is observed with proposed method.

Keywords: ACO, Sobel, Canny, F-Score

1. Introduction

Image edge detection is a prime problem in image segmentation. Edge detection is comprehensively used in various fields of engineering science and technology. An edge can be defined as a group of connected pixels lying between boundaries of two regions. An Edge is a local concept but the boundary is a global concept. The edge pixels are the pixels whose grey levels have big difference with the gray levels of their neighbourhood pixels [1-4]. Edge detection process could be defined as the technique of extracting the edges in a digital image. It is a set of arrangements of actions with the main purpose of identifying points in an image where variations or discontinuities in intensity take place. This set of action is vital to comprehend the substance of an image and with the help of these extracted edge points, we can have the important information in the field of machine vision and image analysis [1]. It goes about as a pre-processing stage for extraction of feature and object recognition [1]. It is generally used in starting phase of computer vision applications. In

*Corresponding sahilraheja78 @gmail.com

biometrics, edges are important to capture important features of biometric identifies. Similar in fog and rain streak detection, edge detection is used to enhance background edges, so that fog and rain streaks can be removed from the images. The traditional methods are based on design of a kernel and depending on type of kernel, various edges are detected either using single or double thresholds [1]. Edge detection is heavily relying on intensity change, and a sharp change in intensity refers to an edge point. In gradient based method we count amplitude changes as

$$c(f) = N\{p \big| |f_p - f_{p-1}| \neq 0\} \tag{1}$$

where p and p - 1 index neighboring samples (or pixels). $|f_p - f_{p-1}|$ is a gradient w.r.t. p in the form of forward difference. $N\{\}$ is the counting operator, outputting the number of p that satisfies $|f_p - f_{p-1}| \neq 0$, that is, the L_0 norm of gradient. In gradient based method both magnitude and directions are important in classifying edge and non-edge pixels.

2. Background

In past various kernels based methods like Canny, Sobel, Robert, Laplacian and Prewitt etc. emerged [1]. These methods successfully find edges in different images. However, in these methods, edge detection is not prefect and in addition to the true edges, they also detect false edges. In fact, false edges are more in number than true edges. Therefore, novel techniques based on swarm intelligent have been proposed. One such technique is Ant Colony Optimization (ACO). This methodology is fundamentally based on the perception of real ant colonies. In early 1990s, this algorithm was presented by M. Dorigo and his colleagues [2]. A comparison of numerous methods of image edge detection of Gradient and Laplacian based edge detection was proposed by R. Maini and H. Aggarwal [3].

Problem: Algorithms that are gradient-based like Sobel, Canny and Prewitt filter etc. have a noteworthy disadvantage of being quite delicate to noise. The size and coefficients of kernel matrix can take fixed set of values and can't be adjusted to a given image. Thus, there is a need of adaptive edge detection algorithms which can provide robust solutions that can make the adjustments as per the changing levels of noise levels of these images to assist in recognizing contents of valid image from visual artifacts presented by noise. Therefore, techniques are needed which are adaptive in nature and which can automatically adjust threshold to produce more correct edges.

Literature Review:

In past, various ACO-based approaches for the edge detection in images and video frames have been proposed [4], [5] and [6]. First attempt for ACO based edge detection technique was proposed in [4], where it is shown that ACO can be successfully used in edge detection. In [5], ACO based technique is used to connect broken edges. In [6] ACO is used to detect edges and contour of an image. In edge detection methods, some kinds of mechanism are used to further enhance the detected edges (refer [7], [8] and [9]). In [7], image pre-processing of image is suggested before applying ACO and other techniques to enhance and then detect edges. In [8] histogram equalization based technique is proposed to further correctly detect edges. In [9] fuzzy based techniques are used for the localization and detection of edges.

Proposed Solution:

However, in ACO based past method, four intensity mapping functions are considered and different images are tested on these functions, and the one which provides descent solution is chosen [4]. Ideally there are uncountable functions to represent various images. Moreover, none of above mentioned papers in past uses any statistical measure to observe the quality of edge detection.

In this paper, we have considered six image from Berkeley Segmentation Dataset which is a notable dataset used in edge detection [4]. For all six images, intensity variations are captured and on the basis of arising variations, a novel intensity mapping function which works well on most of the images is presented. The results are obtained in terms of PSNR (Peak Signal to Noise Ratio), Accuracy and F-measure. PSNR is a measure of quality of images while other two are related with correctly detected edges. The results are shown and compared with old famous Canny and Sobel edge detection methods. Finally, results are also compared with recently proposed other methods in terms of statistical measures.

3. Ant Colony Method and Edge Detection

In this ACO technique, a fixed number of ants which is decided by the size of an image proceed onward a 2-D picture, venturing starting with one pixel then onto the next to build a pheromone matrix, which is used for the identification of edge pixels. The development of the ants is coordinated by the nearby variety of the force values of image [4]. The procedure of image edge detection [4] contains the accompanying steps:

3.1 Initialization Phase

In this procedure for a picture (I : intensity of pixel) I_{MN} (where M and N represents in size) is input information on which ants travel to find solutions. The considered K ants are moved haphazardly over the entire picture with the end goal that the each pixel of the picture is seen as a node. The constant is τ allotted to every, which is the underlying estimation of each part of the pheromone matrix. Initially, each entry of the pheromone matrix $\tau^{(0)}$ is considered as a constant.

3.2. Construction Phase

One ant is irregularly chosen at the n-th construction-step from the K ants, and this ant moves continuously on the image for S steps. The ant movements to its neighboring node (x, y) depends on transition probability and is defined as

$$p^{n}_{(l,m)(x,y)} = \frac{\left(\tau^{(n-1)}_{x,y}\right)^{\alpha} (\eta_{x,y})^{\beta}}{\sum_{x,y\in\Omega_{(l,m)}} \left(\tau^{(n-1)}_{x,y}\right)^{\alpha} (\eta_{x,y})^{\beta}}, \quad y \in \Omega_x \tag{2}$$

In the above equation, for node (x, y), is $\tau^{(n-1)}_{x,y}$ defined as the pheromone value. Parameter $\Omega_{(i,j)}$ represents the neighborhood nodes of the node (imp), the parameter $\eta_{x,y}$ defines the heuristic value at a particular node (x, y). The effect of the pheromone and the heuristic matrix is represented by the constants α and β respectively.

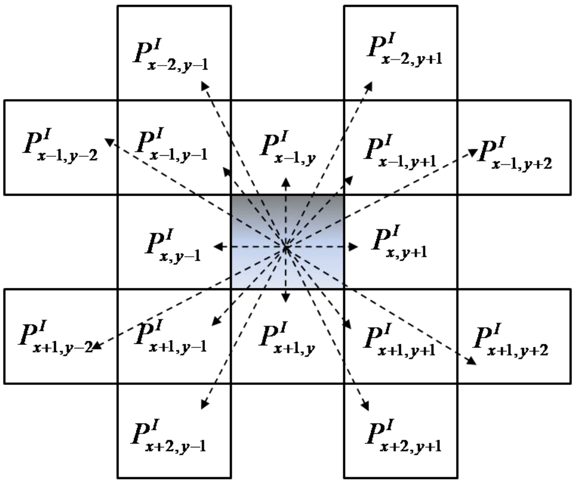

Fig. 1-Pictorial representation of clique

The procedure comprises two vital issues as:

1. Using the inner clique determine the heuristic data)

$$\eta_{x,y} \quad \eta_{x,y} = \frac{1}{Z} G_c(x,y) \tag{3}$$

and

2.

$$Z = \sum_{x=1:M} \sum_{y=1:N} G_c(x,y) \tag{4}$$

The parameter Z is used for normalization, while $P^I_{x,y}$ represents the intensity of the pixel at the (x, y) position of the image I_{MN}, the function $G_c(x, y)$ is a function of a local group of pixels (known as the *clique*), and its estimation relies on the changes in intensity values of image of the clique (as illustrated in Fig .1). For the pixel $P^I_{x,y}$ the function $G_c(x,y)$ is

$$G_c(P^I_{x,y}) = F\begin{bmatrix} \left|P^I_{x-2,y-1} - P^I_{x+2,y+1}\right| + \left|P^I_{x-2,y+1} - P^I_{x+2,y-1}\right| \\ + \left|P^I_{x-1,y-2} - P^I_{x+1,y+2}\right| + \left|P^I_{x-1,y-1} - P^I_{x+1,y+1}\right| \\ + \left|P^I_{x-1,y} - P^I_{x+1,y}\right| + \left|P^I_{x-1,y+1} - P^I_{x-1,y-1}\right| \\ + \left|P^I_{x-1,y+2} - P^I_{x-1,y-2}\right| + \left|P^I_{x,y-1} - P^I_{x,y+1}\right| \end{bmatrix} \tag{5}$$

The proposed intensity mapping function $F(\cdot)$ in above equation is

$$F(x) = \mu x + \sin\left(\frac{\pi x}{2\mu}\right) \qquad \text{for } 0 \le x \le \mu \tag{6}$$

In general, to complete map pixel values of a particular image, $F(x)$ is unique for each image. The proposed function considers two types of variations, one is linear and other is sinusoidal which fit on large number of images as shown in result section. The parameter μ defined in the functions (8) modifies the functions' respective shapes. The acceptable range of the ants movement (i.e., $\Omega_{(i,j)}$ as in equation (4)) is considered to be the 8-connectivity neighborhood, as demonstrated in Fig . 2. The proposed function is further explored in result section.

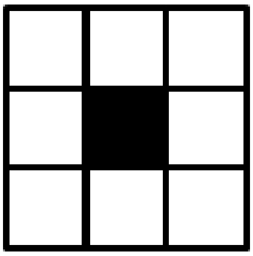

Fig. 2- Schematic of 8-connectivity neighborhood

3.3. Update Phase

In the update process, we update the pheromone matrix after the two operations of updation. The initial update is performed after the mobility of every ant in every development step. Every block of building of pheromone matrix is altered as

$$\tau^{(n-1)}_{x,y} = \begin{cases} (1-\rho)\tau^{(n-1)}_{x,y} + \rho\Delta^k_{i,j} & \text{if } (x,y) \in \text{vca} \\ \tau^{(n-1)}_{x,y} & \text{otherwise} \end{cases} \tag{7}$$

Where, 'vca' means 'visited current ant'. At this point, the parameter ρ, represents the rate of evaporation of pheromone, is estimated using the heuristic matrix. Second update is performed after the completion of the movement of the total ants in each step as

$$\tau^{(n)} = (1-\psi)\tau^{(n-1)} + \psi\tau^{(0)} \tag{8}$$

Now, the parameter ψ represents the pheromone decay coefficient expands the look for the consequent ants by diminishing the pheromone level on the visited edges. Along these lines, it gives a chance to the consequent ants to create fundamental arrangements. Consequently, the probability of reiteration turns out to be more improbable in a similar iteration [10].

3.4 Decision Phase

Finally, at each pixel position, decision has to be made to find out whether it is edge or not, by making application a threshold Th on the basis of last updated pheromone matrix $\tau^{(N)}$. The Th in this research article to be adaptively estimated on the basis of the technique created in [11]. We chose the initial threshold $Th^{(0)}$ as the pheromone matrix mean value. After this following steps are performed:

Step 1: Initialize $Th^{(0)}$ as

$$Th^{(0)} = \frac{\sum_{x=1:M} \sum_{y=1:N} \tau_{x,y}^{(n)}}{MN} \qquad (9)$$

and fix the iteration index as q= 0.

Step 2: Now pheromone matrix $\tau^{(n)}$ is divided into two classes making use of $Th^{(q)}$, here the first class comprises entries of τ which is lesser than threshold $Th^{(q)}$, and the left over entries of τ in other half. After this, make the calculation of the mean of two classes as

$$m_L^{(q)} = \frac{\sum_{x=1:M} \sum_{y=1:N} c\tau_{x,y}^{(n)}}{\sum_{x=1:M} \sum_{y=1:N} \tau_{x,y}^{(n)}} \qquad \text{for}| c \le Th^{(q)} \qquad (10)$$

$$m_U^{(q)} = \frac{\sum_{x=1:M} \sum_{y=1:N} c\tau_{x,y}^{(n)}}{\sum_{x=1:M} \sum_{y=1:N} \tau_{x,y}^{(n)}} \qquad \text{for c} \ge Th^{(q)} \qquad (11)$$

Step 3: Fix the index of iteration q = q+ 1, and we update the threshold as given below

$$Th^{(q)} = \frac{m_L^{(q)} + m_U^{(q)}}{2} \qquad (12)$$

Step 4: In the case of $\left|Th^{q} - Th^{(q-1)}\right| > \varepsilon$, after this move on to *Step 2*; else, the iteration method is discontinued and a decision is made on all pixel's location (x, y) in order to find out edge using:

$$E_{x,y}^{d} = \begin{cases} 1 & \tau_{x,y}^{(n)} \ge Th^{(q)} \\ 0 & \text{elsewhere} \end{cases} \qquad (13)$$

3.5. Proposed Modifications

In the first suggested modification step -3 is modified as

Step 3: Fix the index of iteration q = q+ 1, and we update the threshold as given below

$$Th^{(q)} = \frac{w_1 m_L^{(q)} + w_2 m_U^{(q)}}{2} \qquad (14)$$

Where, w_1 and w_2 are the weights given to both thresholds satisfying $w_1+w_2=1$.

In the second modifications step -4 is defined as:

Step 4: In continuation of step 4, following condition is also included. For each value of w_1 and w_2 threshold is evaluated and F-score is calculated, and finally select the value of w_1 and w_2 for which F-score is maximum.

4. Simulation and Results

The performance of ACO based edge detection method with novel intensity method is done by using computer simulation in MATLAB(R). In the simulation, BSD (Berkeley Segmentation Dataset) is considered. In total, we have considered six images defined as 1-6 (Fig. 3), along-with the ground truth images (g) which contain ideal edges.

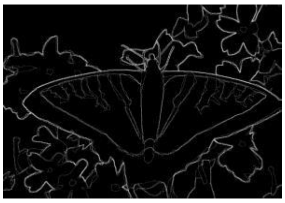

35010 (1)

1(g)

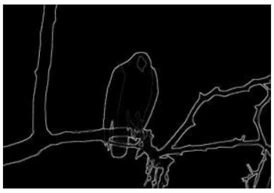

42049 (2)

2(g)

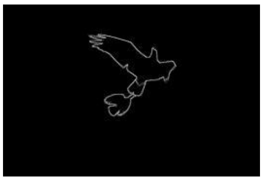

118035 (3)

3(g)

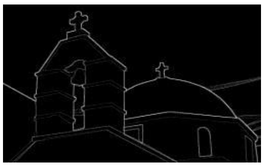

135069 (4)

4(g)

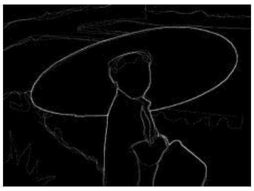

5(g)

189011 (5)

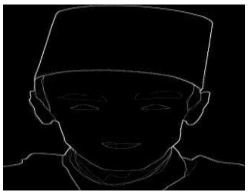

189080 (6)

6(g)

Fig. 3- BSD image database

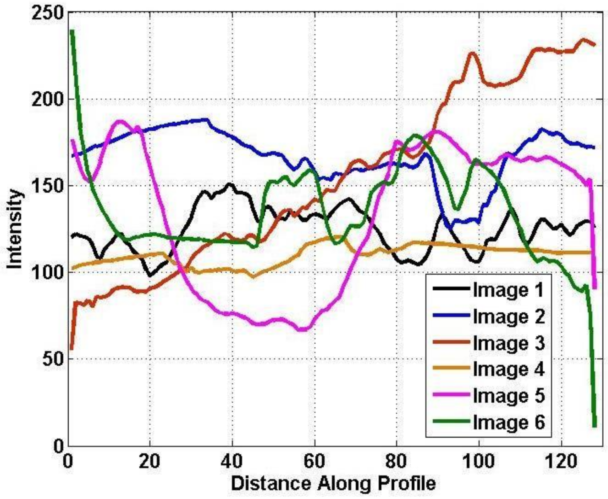

Fig. 4-Intensity profiles for all six images

In Fig. 4, intensity profiles for all six images are shown. In all six profiles, linear and sinusoidal variations can be seen, except in image 6 where a narrow spike can be seen. Thus, images where abrupt profiles changes are seen sinc function will be a better option, but still chosen function fit most of the images with fair accuracy. In particular, image 3 and 4 can be approximated by a linear function; similarly image 1 and 5 can be approximated with sinusoidal function, while image 2 and 6 is well approximated by addition of both linear and sinusoidal function. The difference between exact mapping and approximated function leads to difference of nearly 1.5 to 2.0 dB in PSNR while accuracy affected by 0.5 to 2.5%. We make the calculation of performance on the grounds of PSNR, Accuracy and F-measure. The (PSNR) is given by

$$PSNR = \frac{[255]^2}{MSE} \qquad (15)$$

where:

$$MSE = \frac{[I_g(i,j) - I_o(i,j)]^2}{mn} \qquad (16)$$

In above $I_g(i\ j,\ )$ is ground truth image and $I\ i\ j_o(\ ,\ )$ is image obtained through Sobel, Canny and ACO methods.

The accuracy is defined as

$$Accuracy = \frac{TE}{TE + FE} \qquad (17)$$

where, TE=True Edges
FE=False Edges

This is an important factor and its ideal value is 1, but due to the false detection accuracy goes down, and in fact in many traditional methods more numbers of false edges are detected than true edges.

F- Measure is a test of accuracy, and it is a weight function of precision and recall. In case of equal weightage, it is the harmonic mean of precession and recall.

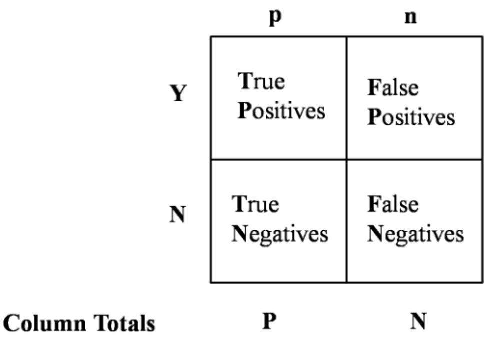

	p	n
Y	True Positives	False Positives
N	True Negatives	False Negatives
Column Totals	P	N

Fig. 5-Characteristic matrix

The important parameters are defined as:

$$P = \frac{TP}{TP + FP}, \quad R = \frac{TP}{TP + FN} \tag{18}$$

Where,
P=Precision
R=Recall
TP=True Positive
FP=False Positive
FN=False Negative
Finally the F-Score is given by

$$F = \frac{2PR}{P + R} \tag{19}$$

Where *P* is total positive, *N* is total negative and so on (Fig. 5). *F*-measure is a test of accuracy, in binary classification. It depends on both precession and recall to get test score. The maximum value of *F* is 1 with minimum as 0.

TABLE 1- Simulations Parameters [4]

Parameters	Value
Total number of construction steps	8
pheromone matrix, τ_{init} (Initial values)	0.0001
Pheromone information, α (Weighting factor)	1
Heuristic information, β (Weighting factor)	0.1
Connectivity neighbourhood, Ω	8
Functions adjusting parameter, μ	10
Total number of ants	vary
evaporation rate, ρ	0.1
Total number of ant's movement-steps, *S*	40
Pheromone decay coefficient, ψ	0.05
Tolerance value, ε	0.1
Threshold, *Th*	adaptive

The simulation parameters are detailed in Table 1. The total numbers of ants which is needed to be taken depends on image size. If image under consideration of size (m×n) than the number of ants are $\left\lfloor \sqrt{mn} \right\rfloor$.

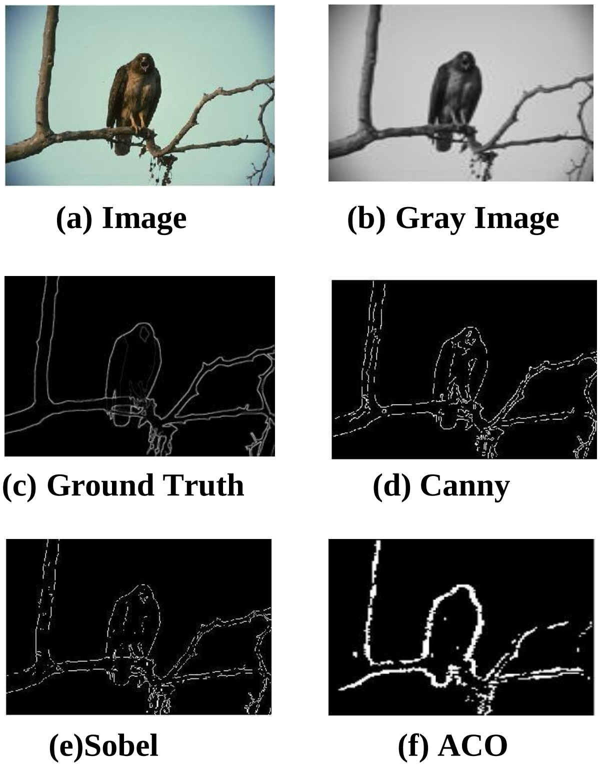

(a) Image (b) Gray Image

(c) Ground Truth (d) Canny

(e)Sobel (f) ACO

Fig. 6-Results comparison of different algorithms

In Fig. 6, six images (a-f) are shown. Images description is also given. If we carefully examine image (d) we observe that it detects most of the true edges but it also detects a large number of false edges. Sobel method tries to discard false edges, but in doing so it also discards true edges (e). However, ACO detects large numbers of true edges with few false edges (f). It is very difficult to judge the quality of image by using human visual system, Therefore, performance measures as discussed above, are used for comparisons of methods. In our work we have shown comparison with Sobel and Canny methods which are still used in edge detection methods, the main aim of choosing these two method is that we want to show that the effectiveness of ACO methods over currently used edge detection methods.

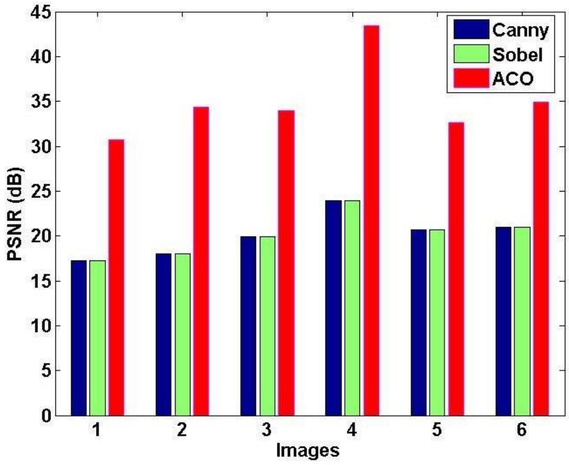

Fig. 7- PSNR comparison for different algorithms

In Fig. 7, PSNR (dB) is plotted for all six images under considerations. In terms of PSNR the performance of Canny and Sobel is nearly same, however in most of cases PSNR is below 20 dB except for image 4 where it is nearly 23.5 dB, which is of poor quality as in image processing a good quality image has PSNR> 30 dB. Thus, the edge detected images are not re-usable when we consider Sobel or Canny detection. While in case of ACO, the PSNR is above 30 dB, in all the cases and for image 4, it is nearly 44 dB which is of excellent quality.

In edge detection accuracy is an important phenomenon, as most of the kernel based method successfully identifies the edges, but in addition to this these methods also detects false edges. Infect, number of false edges is more in comparison to true edges. In Fig. 8, accuracy of different methods are shown, the performance of Canny method is better in comparison to Sobel method, still the accuracy is below 20%. In case of ACO the minimum accuracy is 87%. This happens because with ACO, the numbers of falsely accepted edges are very less sometime in state of confusion ACO reject true edges. Therefore, in ACO the numbers of detected true edges is much more than falsely accepted edges. Thus, accuracy is high.

In Fig. 9, F-score is shown for all six images. For each ground truth image score is 1. In our experiment, Sobel and Canny methods are considered without using any morphological operations. Thus, basic methods are full of errors and F-measure is less than one. However, further improvements are done to improve F-score as detailed in Table. The obtained F-score with ACO is of excellent quality and lies between 0.67 to 0.97.

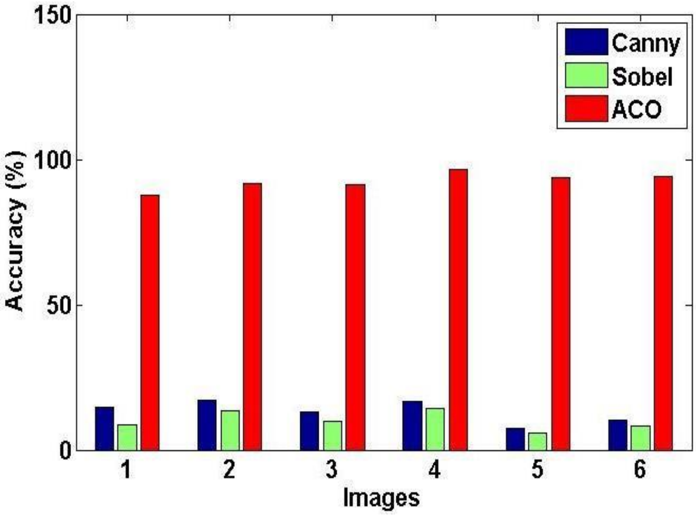

Fig. 8 - Accuracy comparison for different algorithms

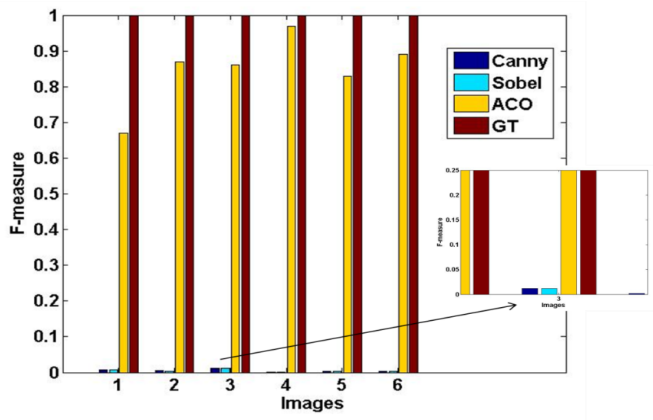

Fig. 9 - F-measure comparison for different algorithms

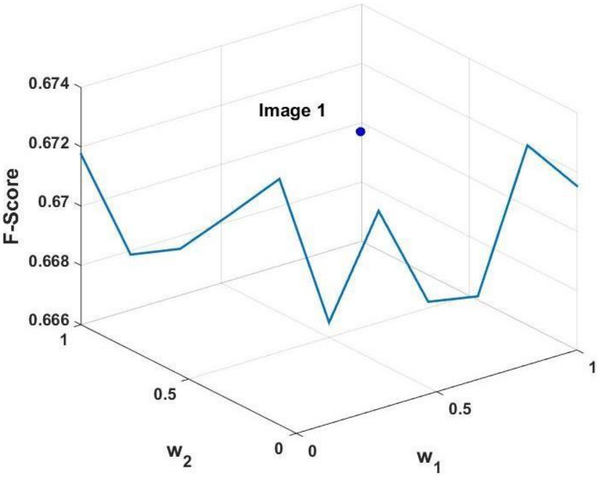

Fig. 10 - F-measure variation for image 1

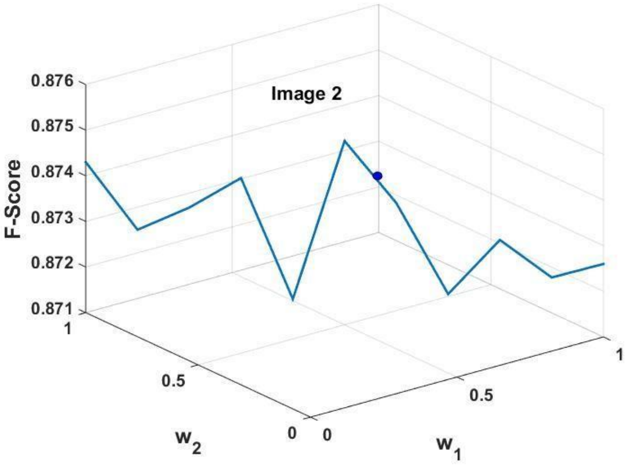

Fig. 11 - F-measure variation for image 2

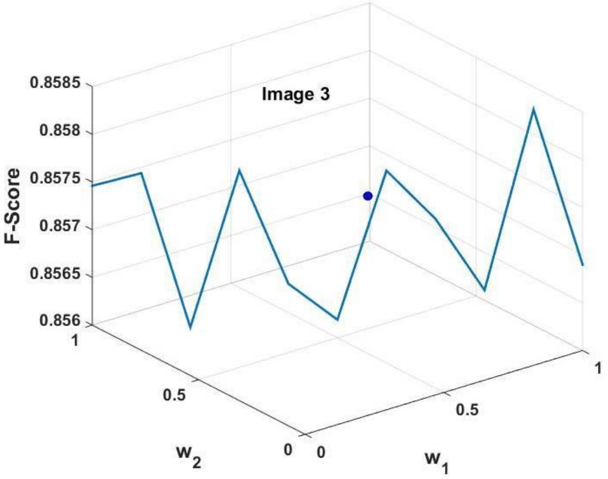

Fig. 12 - F-measure variation for image 3

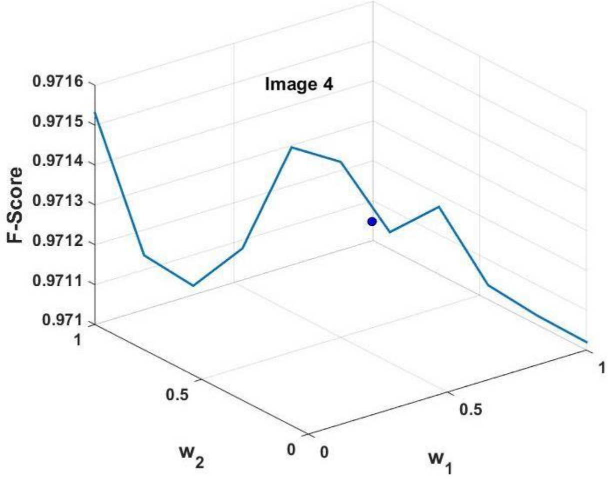

Fig. 13 - F-measure variation for image 4

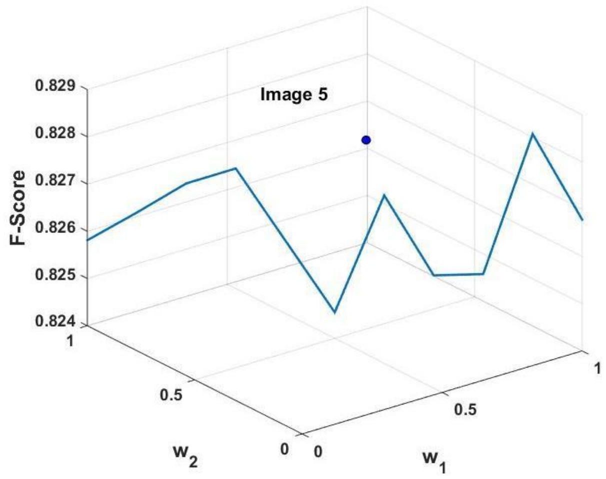

Fig. 14 - F-measure variation for image 5

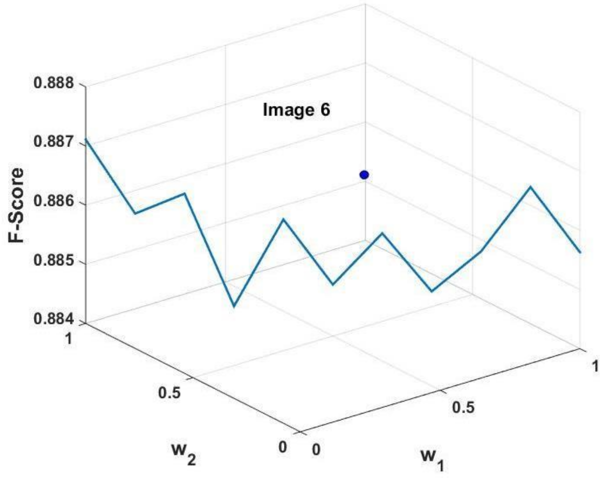

Fig. 15 - F-measure variation for image 6

In Figs. 10-15, F-score variations are shown for all six images. The dot marked on each figure, is the value obtained from previous methods. It is clear from the figures that ups and downs are seen in results but better is comparison to old methods. It is also noticeable that the number of edges in an image are very large in number, therefore a small increment in F-score bring significant improvement in edge detection. In Table 2, for all six images maximum value of F-score along with corresponding values of w_1 and w_2 are shown.

Table 2 - F-Score and Weights

Image	Weight pair (w_1 ,w_2)	F-Score (old, new)
1	[(0,1)	(0.67153, 0.67282)
2	(0.5,0.5)	(0.87325 ,0.87503)
3	[(0.9, 0.1)	(0.85650, 0.85850)
4	(0,1)	(0.97108, 0.97153)
5	(0.9, 0.1)	(0.82623, 0.82854)
6	(0,1)	(0.88510, 0.88711)

5. Analysis

Thus, ACO- based edge detection scheme is a good choice for edge detection. The obtained F-score using other methods proposed recently are shown in Table 3. In the table F-score is presented after applying morphological operations. The F-measure for Canny and Sobel methods are 0.49 and 0.40 respectively. For the BEL method it is 0.63, while for gpb and structure forest is 0.71. For sketch token F-score is 0.73. However, in our case F-score varies from 0.67 to 0.97. It is also noticeable that in our method, we have not used any morphological operations for contour generation and edge joining etc.

Table 3 - Comparison with Notable Works

Methods	Year	F-measure
Canny [12]	[1996]	0.49
Sobel [13]	[2009]	0.40
BEL [14]	[2006]	0.63
gPb [15]	[2011]	0.71
Sketch Token [16]	[2013]	0.73
Structured Forest [17]	[2013]	0.71
ACO	[2018]	0.67-0.97

6. Conclusions

In this paper, an ACO based edge detection method is detailed and obtained results are compared with recently proposed methods. In nut-shell we found the followings:

- In this work we have come up with novel pixel mapping function.
- It has been found that, ACO method is very efficient with average detection accuracy of nearly 87%.
- The F-score is very good and it out-performs the recently proposed methods. The PSNR value is of very good quality.
- The weighted method is effective in maximizing F-scores.
- Sketch Token provides best F-score of 0.73 and with proposed method the obtained best F-score is 0. 97, therefore percentage improvement is of 32.80% is observed with proposed method.

Future Work

The obtained results can be improved using further image processing operation as used in Canny edge detection method. Moreover, method could be searched to make edge detection mechanism free from mapping function by taking into account the gradient magnitude and directions even in ACO based detection. ACO method can be further improved by using fuzzy logic based false edge removals.

Acknowledgement

I would like to thank the reviewers for their valuable comments in improving the quality of this work.

References

[1] Singh RK, Shekhar S, Singh RB, Chauhan V (2014). A Comparative Study of Edge Detection Techniques. International Journal of Computer Applications, 1; 100(19).

[2] Dorigo M, Birattari M, Stutzle T (2006). Ant colony optimization. IEEE computational intelligence magazine, 1, 28-39.

[3] Maini R, Aggarwal H (2009). Study and comparison of various image edge detection techniques. International journal of image processing (IJIP), 1, 1-1.

[4] Tian J, Yu W, Xie S (2008). An ant colony optimization algorithm for image edge detection. In Evolutionary Computation, CEC, 751-756.

[5] Lu DS, Chen CC (2008). Edge detection improvement by ant colony optimization. Pattern Recognition Letters, 29, 416-425.

[6] Gupta C, Gupta S (2013). Edge detection of an image based on ant colony optimization technique. Int. J. Sci. Res.(IJSR). 2, 1256-1260.

[7] Reddy RV, Raju KP, Kumar MJ, Kumar LR, Prakash PR, Kumar SS (2017). Comparative Analysis of common Edge Detection Algorithms using Pre-processing Technique. International Journal of Electrical and Computer Engineering (IJECE)., 7, 2574-2580.

[8] Asharudeen M, Menon HP (2018). Edge detection Using Histogram Localization. Indonesian Journal of Electrical Engineering and Computer Science, 1, 11

[9] Alawad AM, Rahman FD, Khalifa OO, Malek NA (2018). Fuzzy Logic Based Edge Detection Method for Image Processing. International Journal of Electrical and Computer Engineering (IJECE). 8, 1863-1869.

[10] Xiao P, Li J, Li JP (2010). An improved ant colony optimization algorithm for image extracting. In Apperceiving Computing and Intelligence Analysis (ICACIA), International Conference , 17, 248-252.

[11] Otsu N (1979). A threshold selection method from gray-level histograms IEEE transactions on systems, man, and cybernetics. 9, 62-66.

[12] Canny J (1987). A computational approach to edge detection . In Readings in Computer Vision, 184-203.

[13] Vincent OR, Folorunso O. (2009). A descriptive algorithm for sobel image edge detection. In Proceedings of Informing Science & IT Education Conference (InSITE) 40, 97-107.

[14] Dollar P, Tu Z, Belongie S. Supervised learning of edges and object boundaries (2006). In Computer Vision and Pattern Recognition, 2006 IEEE Computer Society Conference, 1964-1971.

[15] Arbelaez P, Maire M, Fowlkes C, Malik J (2011). Contour detection and hierarchical image segmentation. IEEE transactions on pattern analysis and machine intelligence. 33, 898-916.

[16] Lim JJ, Zitnick CL, Dollár P. Sketch tokens (2013): A learned mid-level representation for contour and object detection. In Computer Vision and Pattern Recognition (CVPR), 3, 158-165.

[17] Dollár P, Zitnick CL (2013). Structured forests for fast edge detection. In Computer Vision (ICCV), 2013 IEEE International Conference, 1841-1848.